

Differential tropism of pseudorabies virus for sensory neurons in the cat

J Patrick Card^{1,2}, Lynn W Enquist⁴, Alan D Miller⁵ and Bill J Yates^{1,3}

Departments of ¹Neuroscience, ²Psychiatry, and ³Otolaryngology, University of Pittsburgh, Pittsburgh, Pennsylvania 15260; ⁴Department of Molecular Biology, Princeton University, Princeton, New Jersey 08544; ⁵Laboratory of Neurophysiology, The Rockefeller University, New York, NY, 10021, USA

The permissiveness of cat motor and sensory systems to infection by pseudorabies virus (PRV) was examined. Eight adult cats of both sexes received injections of a virulent strain of PRV (PRV-Becker) into either the diaphragm or neck musculature. Temporal analysis of the replication and transynaptic passage of virus in each experimental paradigm revealed that sensory neurons in the dorsal root ganglia were more susceptible to infection than motor neurons. Only scattered motor neurons displayed productive replication of virus at postinoculation intervals extending to 192 h whereas robust replication of virus in neurons in the dorsal root ganglia and dorsal horn of the spinal cord was apparent as early as 96 h post inoculation. The data demonstrate that functionally distinct populations of neurons in the cat are differentially permissive to infection and transneuronal transport of PRV.

Keywords: alpha herpesvirus; transynaptic infection; dorsal root ganglia; cat

Introduction

Many alpha herpesviruses are characterized by their neurotropism and ability to infect and spread within populations of synaptically-linked neurons. Recognition of these properties and the recent demonstrations of the specificity of transneuronal passage of these viruses has led their use for definition of multisynaptic circuits (Strick and Card, 1992; Card and Enquist, 1994; Enquist, 1994; Loewy, 1995; Ugolini, 1995). Thus, the mechanisms governing the replication and transport of these pathogenic virions within individual neurons and through a multisynaptic circuit have important implications for interpreting data derived from this experimental approach. To date, the majority of tract tracing studies have used either the human pathogen herpes simplex virus (HSV) or a swine alpha herpesvirus known as pseudorabies virus (PRV). Although both viruses have been shown to replicate in a variety of circuits, several reports described differential invasiveness of functionally distinct components of a circuit. As early as 1938, Sabin recognized that PRV spread through trigeminal and autonomic circuitry of the mouse quite efficiently following nasal inoculation, but was apparently incapable of invading the olfactory

system (Sabin, 1938). It has subsequently been shown that some, but not all, strains of PRV have the capacity to invade the CNS via the olfactory nerve in young pigs (McFerran and Dow, 1965; Sabo *et al*, 1969; Wittmann *et al*, 1980; Kritas *et al*, 1995) and other examples of differential invasiveness of PRV or HSV have been identified. For example, Rotto-Perceley and colleagues (1992) reported that neurons in the sympathetic component of the autonomic nervous system are more susceptible to infection by an attenuated strain of PRV than motor neurons innervating somatic musculature. Similarly, we have demonstrated that functionally distinct classes of retinal ganglion cells respond differentially to infection with genetically defined isogenic PRV mutants (Card *et al*, 1991, 1992; Whealy *et al*, 1993; Enquist *et al*, 1994). Barnett and colleagues (1993) demonstrated that HSV type 1 and mouse hepatitis virus produce different patterns of central infection following identical inoculation of the nasal cavity or olfactory bulb, and Ugolini (1992) has shown that the rate of HSV-1 transport to the spinal cord through peripheral nerves of adult rats occurs faster in neurons with smaller caliber axons. In addition, Zemanick and colleagues (1991) have reported that one strain of HSV is transported anterogradely after injection into the motor strip of primate cortex while another strain is only transported in the retrograde direction after identical injection. These and other examples

Correspondence: J Patrick Card
Received 6 June 1996; revised 14 August 1996; accepted 31 August 1996

of differential viral tropism vividly demonstrate that neuroinvasiveness is strain dependent and is an important consideration in the use of alpha herpesviruses for the characterization of multi-synaptic circuits.

Pseudorabies virus is remarkable for the wide range of animals that it can infect. It causes a natural disease in some domestic and wild animals (Wittmann and Rziha, 1989) and, if introduced by injection, can infect a more diverse population of mammals and some birds (Nara, 1982). It is noteworthy that it cannot infect humans, apes, chimpanzees, reptiles and insects by any route. Natural infections seem to occur most often in swine, cattle, sheep, dogs and cats (Gustafson, 1975). However, in a given species, young animals are often more susceptible to PRV disease than are adult animals (Wittmann and Rziha, 1989). Since the anatomy and physiology of neural systems in cats are in many instances well established, it is of particular interest to explore the utility of using PRV for transneuronal analysis in this species.

In the present investigation we have analyzed the invasiveness and patterns of viral replication that occur in the spinal cord following injection of PRV-Becker into the diaphragm or neck musculature of adult cats. Dobbins and Feldman (1994) have characterized the pattern of transneuronal infection in the rat produced by injection of PRV into diaphragm and, as noted earlier, Rotto-Perceley and co-workers (1992) have analysed the invasiveness of this strain of virus in rat motor circuitry. Thus, there is a solid foundation for evaluating the utility of this experimental approach in the cat nervous system. Furthermore, the two systems offer complementary approaches for analysis of factors influencing viral tropism and invasiveness. The diaphragm is characterized by a diffuse motor innervation and few sensory afferents (Balkowiec *et al*, 1995; Corda *et al*, 1965; Duron *et al*, 1978; Gottschall, 1981) whereas the neck musculature is rich in sensory afferents and the motor endplates are more densely concentrated than in the diaphragm (Richmond and Abrams, 1975). The data demonstrate that functionally distinct components of the cat nervous system are differentially susceptible to the productive replication of a virulent strain of PRV following peripheral inoculation.

Results

Peripheral inoculation of adult cats with a virulent strain of PRV initially isolated by Becker (PRV-Becker; Becker, 1967) produced an immunohistochemically detectable productive infection in the spinal cord of all animals. However, the magnitude and pattern of infection was directly dependent upon the route of inoculation, the amount of injected virus and the postinoculation interval.

Only scattered infected motor neurons were observed in the ventral horn of the spinal cord at post inoculation intervals extending to 192 h following injection of PRV-Becker into the diaphragm. In contrast, large numbers of neurons displaying viral antigens were observed in the dorsal root ganglia and dorsal horn of the spinal cord following injection of the virus into neck musculature as early as 96 h post inoculation. The permissiveness of animals to infection did not correlate with the sex of the animal.

Temporal aspects of cellular infection

Infected neurons characteristically exhibited moderate to dense immunoreactivity associated with both the cell soma and proximal dendrites, with the intensity and intracellular distribution of viral antigen reflecting the apparent duration of viral replication. For example, the earliest immunoreactivity was observed in the nucleus of infected neurons, while continued viral replication resulted in the appearance of viral immunoreactivity in the somata and dendrites of infected cells (e.g., compare Figure 3b and c). The early appearance of viral antigen in the cell nucleus correlates with DNA replication and packaging whereas the punctate staining that progressively appears across the somatodendritic compartment denotes sites of envelopment, intracellular trafficking, and transsynaptic passage of virions (Card *et al*, 1993; Whealy *et al*, 1991).

Diaphragm injections

Only scattered infected neurons were observed in the animals in which virus was injected into the diaphragm and all of these cells were confined to the ventral horn of the spinal cord. The distribution of infected neurons observed in these animals is mapped on Figure 1 and photomicrographs of representative examples are illustrated in Figure 2. The largest number of immunoreactive neurons was observed in the longest surviving animals (Cases D4 & D5; see Tables 1 and 2). These animals were inoculated with $0.6-1.2 \times 10^7$ pfu of virus and allowed to survive 192 h. In both cases, we observed scattered infected motor neurons that were occasionally associated with small immunoreactive interneurons (Figure 2). The only difference between these cases was the volume of the inoculum; case D4 was injected with 35 μ l and case D5 received 70 μ l of virus. At shorter postinoculation intervals the number of infected neurons was substantially reduced, even though larger concentrations and volumes of virus were injected into the diaphragm. Only one immunopositive neuron was observed in 151 sections from C5 and C6 of the animal that was inoculated with 172 μ l of virus (2.9×10^7 pfu) and allowed to survive 144 h. Sections of C5 and C6 spinal cord from the two remaining animals injected with PRV-Becker

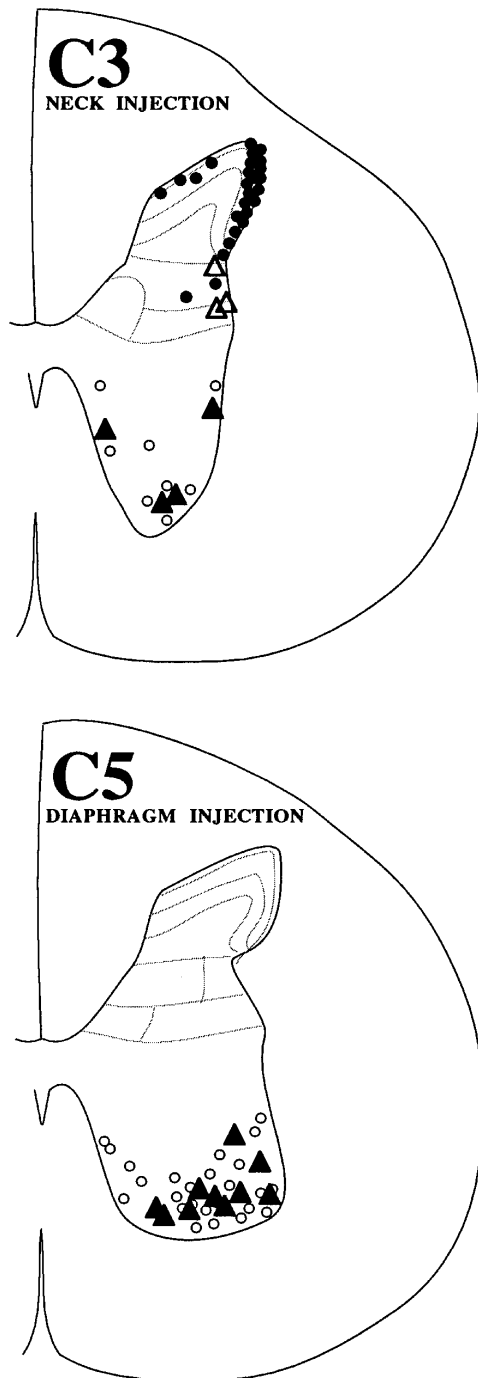


Figure 1 The patterns of infection produced in cervical levels 3 and 5 (C3 & C5) of the spinal cord following injection of the diaphragm (C5) and neck musculature (C3) are illustrated. Each illustration reflects the relative distribution of infected neurons observed in each paradigm; absolute numbers of infected neurons in the different cases are presented in Table 2. Open triangles reflect the position of infected propriospinal neurons and filled triangles mark the location of infected motor neurons. The filled circles illustrate the distribution of infected neurons in laminae I and II of the dorsal horn whereas the small open circles in the ventral horn illustrate the relative position of infected interneurons. Diagrams are adapted from those published by Rexed (1954).

revealed a total of 4 and 14 neurons in a total of 85 and 158 sections, respectively (Table 2). This included one animal inoculated with $172 \mu\text{l}$ (2.9×10^7 pfu) that was sacrificed 96 h post-inoculation and another that received 3.4×10^7 in $201 \mu\text{l}$ and was permitted to survive 72 h. Thus, post-inoculation interval was the most important variable in eliciting a productive infection in this experimental paradigm.

Only 76 neurons were observed in a total of 548 coronal sections though the C5 and C6 levels of the spinal cord (Table 2). The majority of these neurons were confined to the inferior limit of the ventral horn, midway along its mediolateral axis (Figure 1). They displayed two distinct morphologies and, when more than one cell was present in a single section, they were usually found in clusters. Each cluster consisted of a large multipolar motor neuron surrounded by small bipolar neurons (Figure 2a–d). The distribution of immunoreactivity in these neurons was consistent with intermediate to advanced stages of viral replication and there were no cytopathic changes in the infected cells. Nor were there signs of the characteristic infection of glial that has been shown to be associated with lytic changes in neurons infected with PRV-Becker and other strains of PRV after chronic infection of rodent CNS (Rinaman *et al*, 1993). Case D2 demonstrated that infection of the large motor neurons always occurred prior to infection of the small neurons and we never observed infected neurons in the dorsal horn of spinal cord in any of the animals. These observations suggest that infection of smaller neurons in the ventral horn resulted from retrograde transynaptic passage of virus from the first order infection in motor neurons.

The large neurons displaying viral immunoreactivity exhibited a morphology consistent with motor neurons previously shown to innervate the cat diaphragm (Rose *et al*, 1983). The cells exhibited a widest cross sectional diameter of approximately

Table 1 Experimental animals

Animal	Virus	Vol.Inj μl virus/cat	Conc.Inj. pfu $\times 10^7$	Survival (hours)	Level of Spinal Cord Analyzed
D1	PRV-Becker	201	3.4	72	C2, C3, C5, C6
D2	PRV-Becker	172	2.9	144	C5, C6
D3	PRV-Becker	172	2.9	96	C5, C6
D4	PRV-Becker	35	0.6	192	C5, C6
D5	PRV-Becker	70	1.2	192	C5, C6
N1	PRV-Becker	172	2.9	144	C1, C3, C4
N2	PRV-Becker	172	2.9	96	C3
N3	PRV-Becker	70	1.2	120	C1, C3, C4, C5

Details regarding the injection parameters, postinoculation survival intervals and regional analysis conducted in each experiment are provided. D=diaphragm injected animal, N=neck injected animal; C=cervical spinal cord.

50 μm (range=43–65 μm) and were multipolar in conformation (Figure 2a). In cases in which viral replication was more advanced, viral immunoreactivity was apparent in primary and secondary dendrites (Figure 2a and b). Sections adjacent to those exhibiting immunopositive motor neurons often exhibited immunoreactive dendrites in regions approximating the location of the infected perikarya, indicating that the dendritic arbors of infected cells extended radially from the parent neurons (Figure 2b and c). Nevertheless, all immunoreactive dendrites were confined to the gray matter of the ventral horn.

The small infected neurons surrounding these motor neurons were the sole evidence for transynaptic passage of virus in the diaphragm-injected animals. These cells were much smaller than the larger motor neurons and exhibited a distinctly different morphology (Figure 2c and d). The widest diameter of individual cells was approximately 15 μm (range=10–22 μm) and the cell somas were slightly elongated in conformation. In some instances, the presence of viral antigen within the proximal dendrites demonstrated that these cells were bipolar in morphology (Figure 2c and d).

Table 2 Distribution of infected neurons

Animal	SC Level	Total # Sections Analyzed	Sections with infected neurons	Total # of Infected Neurons		
				Laminae I & II	PNs	Ventral Horn
D1	C5	83	8	0	0	6/8
D2	C6	75	0	0	0	0
	C5	73	1	0	0	1/0
D3	C6	78	0	0	0	0
	C5	85	2	0	0	1/3
D4	C5	56	10	0	0	5/37
D5	C5	96	14	0	0	9/7
N1	C3	106	94	1885	5	0
	C4	45	26	67	1	0
N2	C3	109	17	18	0	0
N3	C3	108	100	2052	9	17/119
	C4	41	21	79	2	1/2

Specifics regarding the number and location of infected neurons in each case are provided. The number of neurons in the ventral horn of each level of spinal cord is represented as follows: motor neurons/interneurons. D=diaphragm, N=neck, SC=spinal cord, PN=propriospinal neuron.

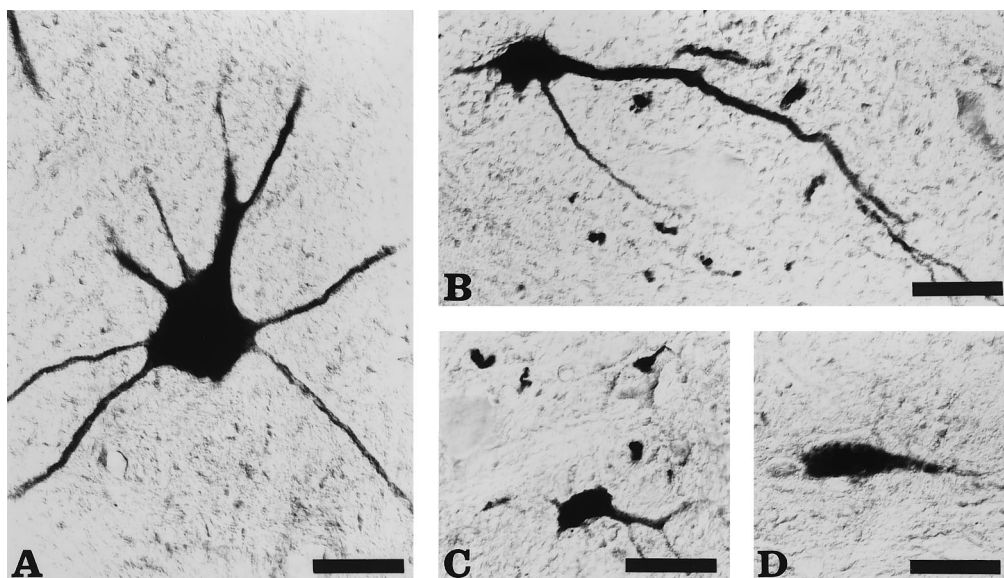


Figure 2 The morphology of infected neurons in the ventral horn of C5 of the spinal cord produced by injection of PRV-Becker into the diaphragm is illustrated. First order infection is restricted to large multipolar neurons with diffusely ramifying dendrites (a and b). Portions of the dendritic arbor of these motor neurons are commonly observed in adjacent sections (arrows in b and c). Retrograde transynaptic passage of virus into the afferents synapsing upon infected motor neurons leads to infection of smaller interneurons in the immediate vicinity of the motor neurons (c and d). Marker bars for a and b=50 μm ; bars for c and d=25 μm .

Injections of neck musculature

Injection of PRV-Becker into the splenius and biventer muscles of the neck resulted in a productive infection of neurons at upper levels of cervical spinal cord in all three experimental animals. The patterns of infection in the spinal cord produced by injection of PRV-Becker into neck musculature differed substantially from that produced by diaphragm injection (Figure 1). All three neck injected animals exhibited infected neurons in lamina I and II of the dorsal horn, but rarely exhibited immunoreactive neurons in the ventral horn (Table 2). The magnitude of infection differed among animals, but the pattern was the same in all cases. A summary of the distribution of infected neurons observed in these cases is shown in Figure 1 and the morphology characteristically exhibited by these cells is illustrated in Figures 3 and 5. Absolute numbers of infected neurons in these regions of spinal cord are

presented in Tables 2 and 3. After injection of 172 μ l (2.9×10^7 pfu) and 96 h survival (case N2) a total of 18 infected neurons were present in 17 of 109 sections from C3 of the spinal cord and these neurons were confined to the superficial laminae ipsilateral to the injection. In contrast, 1890 infected neurons were observed in 94 of 106 sections from the same level of spinal cord 144 h following injection of an equivalent volume of virus (case N1, Table 2). The majority of these cells (1885) were found in the ipsilateral laminae I and II of the dorsal horn, although five cells with a morphology characteristic of propriospinal neurons (see following section for description) were present in laminae V and VI (Figures 3 and 5). The C4 level of the cord in this animal exhibited the same pattern of infection, but the number of infected neurons was substantially reduced (Table 2). No infected neurons were observed in the ventral horn of this animal.

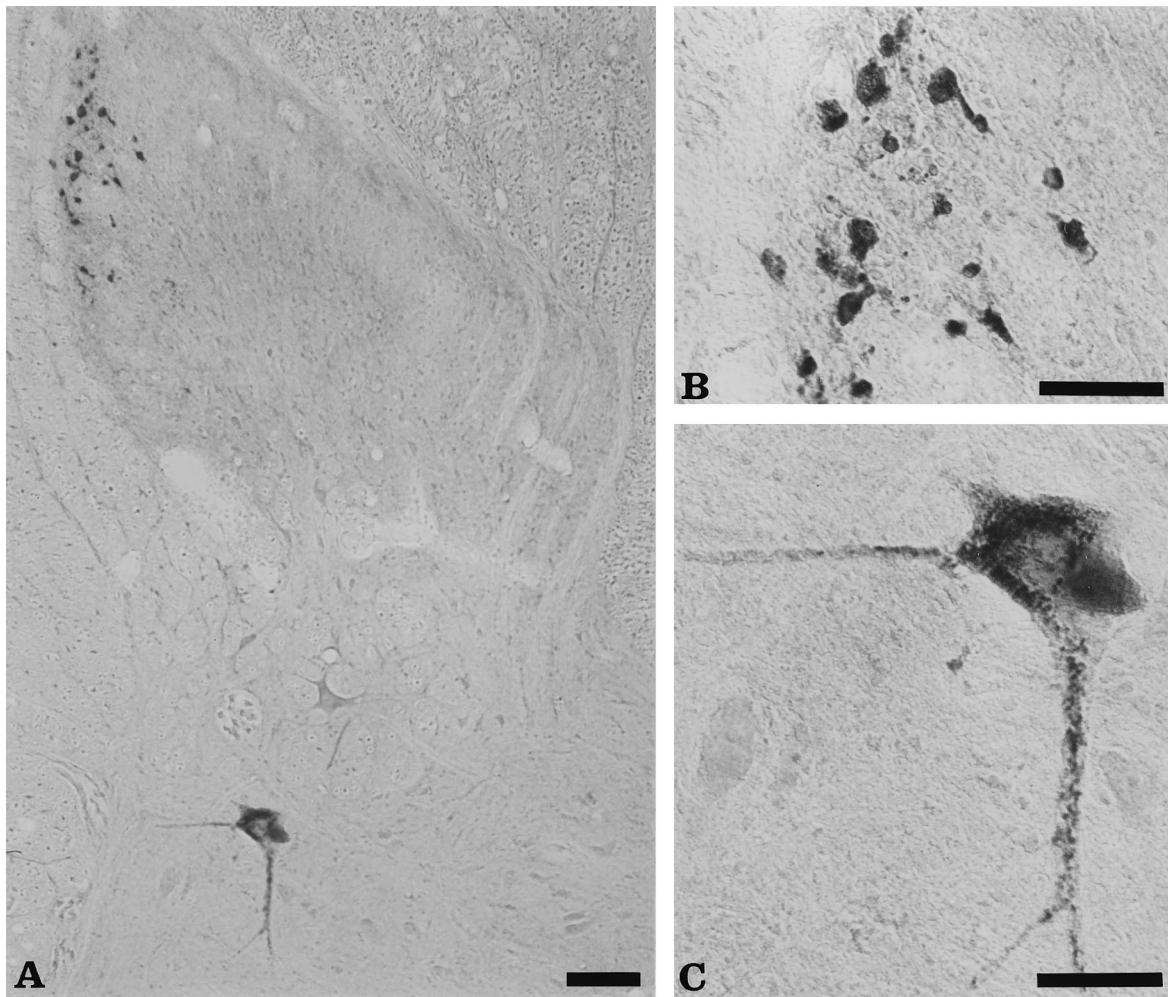


Figure 3 Injection of PRV-Becker into the splenius and biventer muscles of the neck led to a preferential infection of neurons in laminae I, II, V and VII of C3. The general pattern of infection observed in these regions are illustrated in **a**. Small spherical neurons in laminae I and II constituted the largest number of infected neurons (**a** and **b**), but occasional infected neurons in laminae V and VI were also observed (**c**). Marker bar for **a**=100 μ m; bars for **b** and **c**=50 μ m.

Table 3 Distribution of neurons in dorsal horn of C3 after neck injection

Animals	Total # Sections Analyzed	# Sections with ≥ 10 cells/section	Average Number of Neurons in Laminae II & III in Sections with ≥ 10 Infected Neurons		
			Total	Medial	Lateral
N2	106	57	32.33	0.70	31.63
N4	108	75	26.79	3.65	23.12

Details regarding the number of infected neurons present in different regions of laminae I and II of the C3 level of spinal cord in two of the neck injected animals (N2 and N4) are provided.

Case N3, in which the animal was sacrificed 120 h after injection of 1.2×10^7 pfu of virus in 70 μl , also exhibited a large number of infected neurons in laminae I and II of the ipsilateral dorsal horn and occasional infected cells in laminae V and VI; 2052 infected neurons were observed in the superficial laminae of C3 and 9 cells exhibiting propriospinal neuron morphology were present in deeper layers. Again, the pattern of infection in C4 was similar to that seen in C3, but the number of cells was substantially reduced (Table 2). Unlike case N1, a substantial number of PRV-immunoreactive neurons were present in the medial segments of laminae I and II and scattered infected neurons were present in the ventral horn, primarily at the ventral and medial extent of the gray matter (Figure 1b). The morphology of the latter group of neurons was similar to both motor neurons and interneurons, with the number of interneurons exceeding that of the motor neuron population (Table 2).

The pattern of infection produced in the spinal cord by injection of virus into the splenius and biventer muscles also exhibited evidence of topographical segregation of neurons within subfields of laminae I and II. This was true of all cases, but was more apparent in the two animals in which the spinal cord infection was more advanced. The principal characteristic of this topography was the segregation of the majority of infected cells within the lateral half of the dorsal horn (Figures 1, 3a, 5a and b). Furthermore, the presence of large numbers of infected neurons in some sections, considered with the very low number of infected cells in other sections from the same segment of spinal cord, suggested that infected neurons occurred in groups along the longitudinal axis of individual spinal cord segments. For example, of the 106 sections from C3 that were analyzed in case N1, approximately half (49) had fewer than 10 infected cells per section (Table 3). The remaining sections containing an average of 32.33 infected dorsal horn neurons per section and, of that population, less than one cell per section was found in the medial half of laminae I/II. A similar preponderance of infected neurons in the lateral half of laminae I and II was evident in case N3 (Table 3). However, there were

more neurons in the medial portion of laminae I and II in this case and occasional infected neurons were observed in the ventral horn (Figure 5a and b; Table 2).

Examination of sections through the C3 dorsal root ganglion of case N4 ipsilateral to the viral injection demonstrated numerous infected neurons (Figure 4a). Six hundred and fifty-one infected neurons were observed in 17 sections through the ganglion. These cells exhibited an average cross sectional diameter of 41.37 μm (range=30–61 μm ; $n=144$) and they were distributed throughout the ganglion. Photomicrographs illustrating the distribution and morphology of the neurons from this case are shown in Figure 4a–c.

The infected neurons in the spinal cord dorsal horn exhibited two distinct morphologies. Those in laminae I and II presented a very homogenous morphology. They were generally spherical in shape and exhibited a widest diameter of approximately 14 μm (range=10–19 μm) (Figure 3b). Only on rare occasions did the viral immunoreactivity extend into proximal dendrites of these cells and in those instances they presented a bipolar conformation. Infected neurons in laminae V and VI presented a more complex morphology (Figure 5a and b). They were substantially larger than infected neurons in superficial laminae with a widest diameter of approximately 60 μm (range=52–78 μm). In addition, viral immunoreactivity routinely extended well into the dendritic tree of these neurons revealing three to five primary dendrites that radiated away from the cell soma and gave rise to smaller branching secondary and tertiary dendrites. Apical branches of the larger dendrites extended dorsolaterally into laminae I and II where they were often coextensive with infected neurons within these regions. The remaining dendrites extended radially from the multipolar perikarya, but exhibited a preferential trajectory back into the gray matter of the cord (Figure 5a and b).

Discussion

While the cat is reported to be a host for PRV (Nara, 1982), our data demonstrate a dramatic difference in the permissiveness of motor and sensory systems

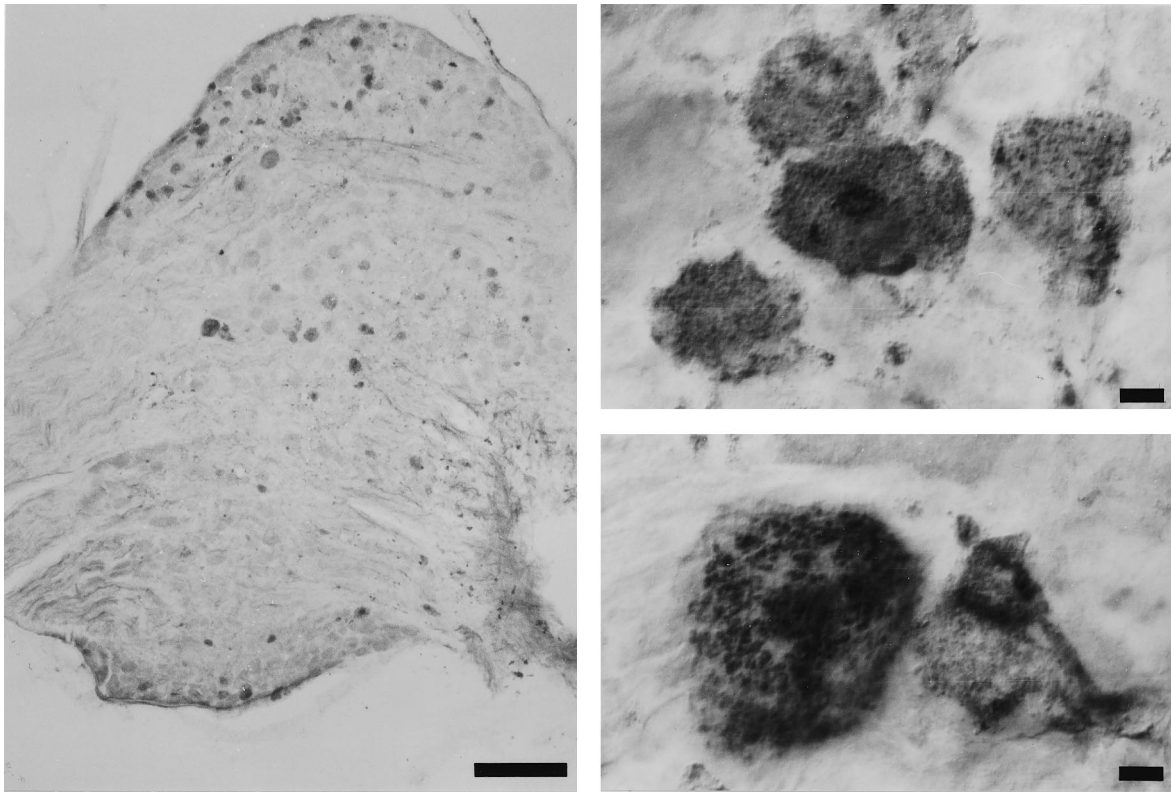


Figure 4 Injection of neck musculature also infected large numbers of neurons in the C3 dorsal root ganglion. (a) illustrates the distribution of infected neurons in a longitudinal section through the ganglion; the cells marked by the arrows in a are illustrated at higher magnification in b and c. Marker bar a=200 μ m; marker bars b and c=10 μ m.

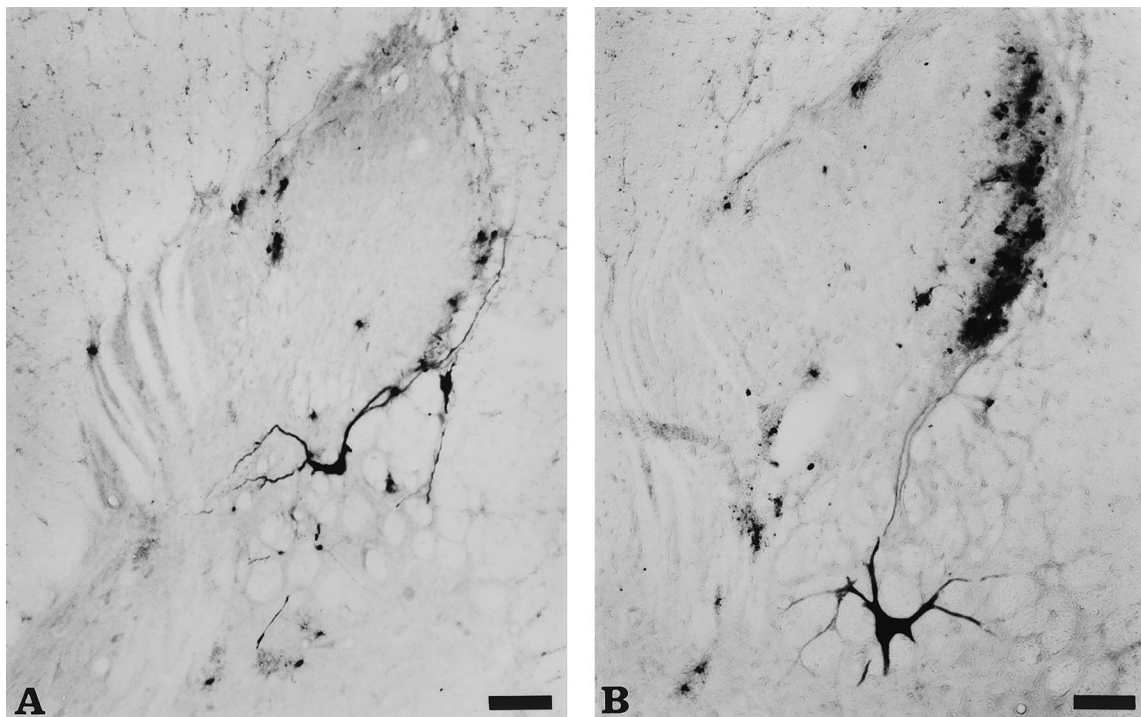


Figure 5 The morphology typical of that displayed by infected laminae V and VI neurons after injection of neck musculature is illustrated in these figures. Note the multipolar perikary giving rise to a prominent primary dendrite that extends dorsolaterally into the region of laminae I and II that contain the largest concentration of infected neurons. Marker bars=100 μ m.

of the cat spinal cord to infection with PRV. Motor neurons innervating both the diaphragm and neck musculature were relatively resistant to viral infection following inoculation with large concentrations of PRV-Becker and long postinoculation intervals. In contrast, small doses of PRV-Becker and shorter postinoculation intervals produced a robust transneuronal infection of dorsal horn neurons in regions previously shown to receive projections from the DRG. Furthermore, the observed patterns of viral replication in the DRG and superficial laminae of the dorsal horn suggested a differential tropism of PRV-Becker for DRG neurons with small caliber axons.

The underlying mechanisms that account for this preferential tropism of PRV for sensory neurons in the cat remain to be defined. Nevertheless, some aspects of our findings combined with those of previous studies provide interesting insights. PRV infection of neonatal animals is usually more devastating than infection of adult animals. Moreover, PRV has a predilection to infect sensory pathways in adult animals, often leading to establishment of latency in sensory ganglia (Wittmann and Rziha, 1989). One particularly noteworthy aspect of our data is the fact that productive replication of virus was largely restricted to sensory DRG neurons and their synaptic targets in the dorsal horn of the spinal cord. As noted earlier, following intranasal inoculation of PRV in adult mice, Sabin (1938) described the preferential spread of virus through trigeminal and autonomic pathways, but failed to observe propagation of the virus in olfactory systems. Although recent studies demonstrate that some strains of PRV can gain access to the CNS via the olfactory nerves, these studies were conducted in young pigs (McFerran and Dow, 1965; Sabo *et al.*, 1969; Wittmann *et al.*, 1980; Kritas *et al.*, 1995). In adult animals, intranasal inoculation of PRV generally leads to establishment of a latent infection of sensory trigeminal neurons rather than productive replication and invasion of the CNS. Although one must be cautious in generalizing properties of infection across species and in different neuronal systems, our findings are consistent with the natural tropism of the virus for sensory fibers in the adult animals. Injection of virus into neck musculature produced a robust replication of virus in the DRG and transynaptic infection of dorsal horn neurons known to receive sensory input from DRG neurons, whereas only occasional viral replication was observed in motor neurons in these animals and those in which the virus had been injected into the diaphragm. The absence of infection in the dorsal horn following injection of the diaphragm is consistent with the demonstrated sparse distribution of a sensory innervation to this muscle. Free sensory endings and Pacinian corpuscles are widely scattered over the surface of the muscle and there are few muscle

spindles and Golgi tendon organs that are confined primarily to the crural region (Balkowiec *et al.*, 1995; Corda *et al.*, 1965; Duron *et al.*, 1978; Gottschall, 1981). Our paradigm did not involve injection of the crus.

The infection of the DRG and dorsal horn of spinal cord in neck injured animals was further distinguished by the differential concentration of viral antigens in a subset of sensory neurons. Examination of the DRG in case N3 demonstrated that only a subpopulation of DRG neurons exhibited viral immunoreactivity and that these cells are distinguished by their small cross-sectional diameter compared to uninfected perikarya. In addition, the transneuronal infection of the synaptic target of these neurons in the dorsal horn of spinal cord was largely confined to the lateral half of laminae I and II, and further appeared to be segregated within groups distributed along the rostrocaudal extent of the C3 level of spinal cord. All of these observations are consistent with virus preferentially infecting small caliber sensory axons innervating the region of the axial neck musculature near the multiple sites of inoculation. Small caliber A δ and C fibers arising from small DRG sensory neurons are known to arborize within the superficial laminae of this region of spinal cord in a pattern that conforms to the distribution of infected neurons observed in our analysis (Willis and Coggeshall, 1991). The infected neurons in laminae V, VI and VII of the C3 level of spinal cord are similar in morphology to propriospinal neurons thought to play an important role in postural adjustments associated with targeted movements (Alstermark *et al.*, 1987, 1991). These neurons are known to receive descending inputs from the cortex, tectum and brainstem as well as afferent input from the forelimb (Illert *et al.*, 1978; Alstermark *et al.*, 1984). Since these neurons exhibited dendrites that extended into the lateral extent of laminae I and II it is probable that they become infected via monosynaptic transneuronal passage of virus from sensory afferents.

Although productive replication of PRV-Becker was largely confined to a subset of sensory neurons, we did observe a limited number of infected motor neurons. This raises the issue of why we did not observe more extensive infection of motor and sensory systems following inoculation of either diaphragm or neck musculature. Particularly germane to this discussion are recent studies of the replication of HSV-1 (Ugolini, 1992) and PRV-Bartha (Rotto-Perceley *et al.*, 1992) in motor circuitry. Ugolini demonstrated extensive infection of both sensory, autonomic and motor systems following injection of HSV-1 into crushed mixed nerves innervating the forelimb on hindlimb of rats (Ugolini, 1992). However, the data from that study also revealed temporal differences in the rate of infection of functionally distinct components of

these mixed nerves. Productive replication of virus in sensory and autonomic neurons with small caliber axons preceded that of motor neurons and sensory neurons with large myelinated axons. This finding suggests that the restricted pattern of infection observed in our analysis may reflect differing rates of viral replication and/or transport in different types of neurons. However, our findings suggest that species specificity and a restricted permissiveness to infection may have also contributed to the preferential infection of sensory systems in the cat. In both of our paradigms, the majority of motor neurons were consistently resistant to productive replication of PRV-Becker even in circumstances in which animals were injected with large concentrations of virus and permitted to survive as long as 8 days. While one might argue that the sparseness of the terminal distribution across the surface of the diaphragm contributed to our failure to infect substantial numbers of phrenic motor neurons (i.e., neurons did not accumulate enough virus to elicit a productive infection), this explanation does not explain the small number of infected motor neurons resulting from injection of large amounts of virus into neck musculature. Unfortunately, the sensory irritation that accompanied the early infection of small DRG neurons precluded analysis of longer surviving animals in this paradigm. Thus, we cannot exclude the possibility that large numbers of motor neurons would have become infected at longer post inoculation intervals. However, it is also important to consider the differences in the method of inoculation in comparing our findings and those of Ugolini (1992). Whereas Ugolini injected virus directly into crushed peripheral nerves, we injected virus into peripheral targets. This suggests that the peripherally projecting axons of motor neurons may not be as permissive to virion invasion as those of sensory terminals. Alternatively, the induction of a productive replication of virus in motor neurons may require higher intracellular concentrations of virus. Resolution of this issue would require injection of virus into the neck musculature of animals that had previously received dorsal root section to eliminate transport of virus into the spinal cord through sensory fibers.

The possibility that motor neurons are more resistant to infection by PRV than other systems is also supported by the findings of Rotto-Perceley and colleagues (1992). These investigators reported that the ability of PRV-Bartha to infect motor neurons innervating the gastrocnemius muscle of the rat was less efficient than the ability of the virus to invade and replicate within autonomic circuitry. The experimental paradigm employed by these investigators was similar to that used in our study in that they injected virus into multiple sites in the muscle. However, the amount of injected virus was far less than used in the present study (1×10^4 pfu *versus*

$1.2 - 2.9 \times 10^7$ pfu) and they used the attenuated Bartha strain rather than the virulent Becker strain of PRV. Using this approach these authors reported that they were successful in infecting sympathetic preganglionic neurons in approximately 90% of animals, but only infected ventral horn motor neurons in about 60% of the injected rats. Analysis of the DRGs and sectioning of the dorsal roots in that study also revealed that virus did not replicate in DRG sensory neurons and they did not observe the pattern of infection in the dorsal horn that we have documented in this study. Certainly, some of the differences observed in our findings and those of Rotto-Perceley and co-workers can be attributed to the different strains of virus employed, and this important difference should be carefully considered in interpreting the data derived from both studies given the results from prior investigations that have documented differences in the neuroinvasiveness and replication of PRV-Becker and PRV-Bartha (Card and Enquist, 1995). Nevertheless, the findings of both studies provide compelling evidence that the tropism of PRV for motor systems is substantially less than it is for other neuronal systems.

Although our injections of diaphragm only infected a small number of phrenic motor neurons there was limited transynaptic passage of virus from these neurons into local circuit premotor neurons. Interneurons with a variety of respiratory-related discharge patterns have been recorded during electrophysiological studies at the same spinal level as the phrenic motor pool in cats and rabbits (Bellingham and Lipski, 1990; Douse and Duffin, 1993; Grelot *et al*, 1993; Palisses *et al*, 1989). Inhibitory connections have been observed between C5 expiratory interneurons and phrenic motoneurons (Douse and Duffin, 1993), but the possible connections between other subtypes of C4–6 respiratory interneurons and phrenic motoneurons have not been examined. Bellington and Lipski (1990) have reported respiratory interneurons are widely distributed around the phrenic nucleus while Douse and Duffin (1993) described the C5 expiratory interneurons being located predominately dorsomedial to the phrenic motor pool. In our analysis, infected ventral horn interneurons were found in the immediate vicinity of the motor neurons from which they were presumably infected via retrograde transynaptic passage of virus, a finding that is consistent with the distribution characterized in rat by Dobbins and Feldman (1994) using transneuronal tracing with PRV.

In conclusion, we have demonstrated that the neurotropism of PRV places a number of constraints upon its use for transneuronal analysis in the cat. The initial goal of our study was to examine the morphological substrates of vestibular influences upon respiratory outflow and of non-respiratory inputs to the phrenic motor pool.

Previous analysis by Yates and colleagues (1993) demonstrated vestibulo-respiratory and vestibulo-sympathetic responses in decerebrate cats, but the precise organization of neurons that mediate these responses has not been defined in this species. Studies of this circuitry in rats by Dobbins and Feldman (1994) had shown that rat phrenic motor neurons are capable of replicating and transporting PRV-Bartha, but did not reveal a monosynaptic projection to these cells from either the medial or lateral vestibular nuclei. Thus, the apparent resistance of cat motor neurons to PRV infection, combined with the permissiveness of sensory neurons to the replication and spread of the virulent Becker strain of PRV was an unexpected finding that further emphasizes the need for thorough parametric analysis before using these neurotropic pathogens for transneuronal analysis of neural circuitry. The data also provide a vivid example of how the tropism of this virus changes in different species.

Materials and methods

Virus

The virulent Becker strain of pseudorabies virus (PRV-Becker; Becker, 1967) was used in this analysis. Virus was propagated on PK15 cells as previously described (Card and Enquist, 1994) to a titer of 1.7×10^8 plaque forming units per milliliter (pfu/ml).

Antisera

Tissue from animals injected with PRV was processed using rabbit polyvalent antisera raised against acetone inactivated virus (Card *et al*, 1990). In prior studies we demonstrated that these antisera produce robust staining of virally infected neurons and are specific for PRV (Card and Enquist, 1994). In the present investigation we incubated sections in a 1:10 000 dilution of primary antiserum for 24–48 h and localized viral immunoreactivity with the avidin-biotin modification (Hsu *et al.*, 1981) of Sternberger's peroxidase-antiperoxidase procedure (Sternberger, 1979). The reagents included affinity purified donkey antirabbit secondary antisera (Jackson ImmunoResearch Laboratories) and the Vectastain Elite Kit (Vector Laboratories).

Experimental animals

Eight adult antibody-free cats of both sexes were used in the analysis. These 'Antibody Profile Defined (APD) Felines' were purchased from Harlan Sprague Dawley, Incorporated (Indianapolis, Indiana). They are unvaccinated and barrier-reared to assure freedom from disease or humoral antibodies affecting disease susceptibility and progression. Upon delivery to the laboratory the animals were maintained in isolation for a brief period of acclimation prior to injection of virus. Injected

animals recovered in individual hepa-filtered cages maintained within an isolated room equipped with a dedicated air supply. The laboratory and procedures used for these experiments met the criteria for Biosafety Level 2 experiments as stipulated in Health and Human Services Publication #88-8395 entitled *Biosafety in Microbiological and Biomedical Laboratories*. The experimental protocol was approved by the Animal Care and Use Committees at Rockefeller University and the University of Pittsburgh.

Animal surgery

All surgery was performed under aseptic conditions in a sterile operating room. Four animals were sedated by intramuscular injection of 0.3 mg/kg acepromazine and 0.15 mg/kg butorphanol. An intravenous catheter was then inserted and the animals were maintained under deep sodium pentobarbital induced anaesthesia. A 25 mg/kg dose was delivered immediately following insertion of the canula; supplementary doses were administered as needed to maintain areflexia. The other animals were anaesthetized using isoflurane vaporized in oxygen; the anesthetic concentration was adjacent to maintain areflexia during the surgical procedures.

Five animals received injections into the left costal region of the diaphragm through an incision in the abdominal wall. Three animals received injections into the splenius and biventer muscles, exposed by an incision through the skin on the dorsal aspect of the left side of the neck at levels C1 to C3 of the vertebral column. All animals received multiple injections of 1 to 2 μ l into each target tissue to achieve final injected volumes ranging from 35–201 μ l of virus per animal (5.9×10^6 pfu to 3.4×10^7 pfu). This amount of injected virus produces a productive infection in 100% of rodents (Card *et al.*, 1995). After inoculation the skin was sutured and the animals were returned to their cage for the balance of the experiment. Further information regarding the amount and type of injected virus, the site of injection, the postinoculation interval, and the regions of spinal cord analyzed in each animal is indicated in Table 1.

Tissue fixation and processing

At the conclusion of each experiment animals were deeply anesthetized with an intraperitoneal injection of sodium pentobarbital (40 mg/kg) and perfused transcardially with phosphate-buffered saline followed by the paraformaldehyde-lysine-sodium metaperiodate (PLP) fixative developed by McLean and Nakane (1974). Segments of cervical spinal cord and, in some cases, their associated dorsal root ganglia (DRG) were postfixed for 1 h at 4°C, washed in 0.1 M sodium phosphate buffered saline (PBS), cryoprotected by immersion in phosphate buffered 20% sucrose solution, and sectioned in the coronal

plane with a sliding microtome equipped with a tissue freezing unit. The spinal cord was cut at 35 μm and dorsal root ganglia (DRG) were cut in the longitudinal plane at 40 μm per section. Tissue was collected serially in 12 bins of PBS and stored at 4°C. One bin of tissue from each level of spinal cord was immediately processed for immunohistochemical localization of viral immunoreactivity to determine the extent of viral replication and transport through motor and sensory circuitry in the spinal cord. The remaining bins were transferred to cryoprotectant and stored at -20°C to preserve antigenicity (Watson *et al.*, 1986). Some of these bins were subsequently processed for viral immunoreactivity to permit analysis of the distribution of infected cells in a more frequent series of sections. The minimum frequency of analysis of each level of spinal cord was 420 μm and, in most cases, a more frequent series of sections was examined.

Analysis of tissue

Each case was analyzed to determine both the distribution and extent of viral replication in coronal sections through the appropriate level of spinal cord or in longitudinal sections through the DRG. Each section of tissue was examined with a Nikon Optiphot photomicroscope to determine the relative distribution and extent of infection. A precise map of the distribution and number of infected neurons in each section was obtained by recording the positions of infected neurons on a camera lucida schematic map produced with a Nikon Optiphot photomicroscope equipped with a drawing tube. The number of neurons in specific regions of the dorsal and ventral horns were then counted. The distribution and size of infected

neurons in the C3 dorsal root ganglion of one of the long surviving PRV-Becker injected animals (N4; see Table 1) were also determined. The location of infected neurons in seventeen 40 μm sections through the ganglion were mapped using a 4 \times objective and the perimeter of each cell was traced.

The widest diameter of a subset of neurons in the DRG and spinal cord was measured using a micrometer scale and a drawing tube. The scale was projected through the drawing tube using a 20 \times objective and recorded on a piece of paper. Infected neurons were then identified on the photomicroscope at the same magnification and the scale was superimposed upon the cell soma using the drawing tube to determine the widest diameter. Only infected cells displaying viral immunoreactivity throughout the cell soma were included in this quantitative analysis. Cells displaying pathological changes were excluded.

For the purposes of illustration, the distribution of infected neurons was mapped upon schematic diagrams of the appropriate level of spinal cord adapted from Rexed (Rexed, 1954). Photomicrographs of infected neurons were taken with a Zeiss Axiophot photomicroscope equipped with differential interference contrast optics.

Acknowledgements

This work was supported by NIH RO1s MH53574 (JPC), NINDS 33506 (LWE), DC00693 (BJY), NS20585 (ADM) and DC02644 (ADM). We gratefully acknowledge the expert technical assistance of Jen-Shew Yen.

References

- Alstermark B, Isa T, Tantisira B (1991). Integration in descending motor pathways controlling the forelimb in the cat. *Experimental Brain Research* **84**: 561–568.
- Alstermark B, Kummel H, Pinter MJ, Tantisira B (1987). Branching and termination of C3-C4 propriospinal neurones in the cervical spinal cord of the cat. *Neuroscience Letters* **74**: 291–296.
- Alstermark B, Lundberg A, Sasaki S (1984). Integration in descending motor pathways controlling the forelimb in the cat. II. Inhibitory pathways from higher motor centres and forelimb afferents to the C3-C4 propriospinal neurones. *Experimental Brain Research* **56**: 308–322.
- Balkowiec A, Kukula K, Szulczyk P (1995). Functional classification of afferent phrenic nerve fibers and diaphragmatic receptors in cats. *Journal of Physiology (London)* **483**: 759–768.
- Barnett EM, Cassell MD, Perlman S (1993). Two neurotropic viruses, herpes simplex virus type 1 and mouse hepatitis virus, spread along different neural pathways from the main olfactory bulb. *Neuroscience* **57**: 1007–1025.
- Becker CH (1967). Zur primären Schädigung vegetativer Ganglien nach Infektion mit dem Herpes suis Virus bei verschiedenen Tierarten. *Experientia* **23**: 209–217.
- Bellingham MC, Lipski J (1990). Respiratory interneurons in the C5 segment of the spinal cord of the cat. *Brain Research* **533**: 141–146.
- Card JP, Dubin JR, Whealy ME, Enquist LW (1995). Influence of infectious dose upon productive replication and transynaptic passage of pseudorabies virus in rat central nervous system. *Journal of NeuroVirology* **1**: 349–358.
- Card JP, Enquist LW (1994). Use of pseudorabies virus for definition of synaptically linked populations of neurons. *Methods in Molecular Genetics* **4**: 363–382.
- Card JP, Enquist LW (1995). Neurovirulence of pseudorabies virus. *Critical Reviews in Neurobiology* **9**: 137–162.

- Card JP, Rinaman L, Lynn RB, Lee B-H, Meade RP, Miselis RR, Enquist LW (1993). Pseudorabies virus infection of the rat central nervous system: Ultrastructural characterization of viral replication, transport, and pathogenesis. *Journal of Neuroscience* **13**: 2515–2539.
- Card JP, Rinaman L, Schwaber JS, Miselis RR, Whealy ME, Robbins AK, Enquist LW (1990). Neurotropic properties of pseudorabies virus: Uptake and transneuronal passage in the rat neuronal system. *Journal of Neuroscience* **10**: 1974–1994.
- Card JP, Whealy ME, Robbins AK, Enquist LW (1992). Pseudorabies virus envelope glycoprotein gI influences both neurotropism and virulence during infection of the rat visual system. *Journal of Virology* **66**: 2032–2041.
- Card JP, Whealy ME, Robbins AK, Moore RY, Enquist LW (1991). Two alpha-herpesvirus strains are transported differentially in the rodent visual system. *Neuron* **6**: 957–969.
- Corda M, von Euler C, Lennerstrand G (1965). Proprioceptive innervation of the diaphragm. *Journal of Physiology (London)* **178**: 161–177.
- Dobbins EG, Feldman JL (1994). Brainstem network controlling descending drive to phrenic motoneurons in rat. *Journal of Comparative Neurology* **347**: 64–86.
- Douse MA, Duffin J (1993). Axonal projections and synaptic connections of C5 segment expiratory interneurons in the cat. *Journal of Physiology (London)* **470**: 431–444.
- Duron B, Jung-Caillol MC, Marlot D (1978). Myelinated nerve fiber supply and muscle spindles in the respiratory muscles of the cat: a quantitative study. *Anatomy and Embryology* **152**: 171–192.
- Enquist LW (1994). Infection of the mammalian nervous system by pseudorabies virus (PRV). *Seminars in Virology* **5**: 221–231.
- Enquist LW, Card JP (1996). Pseudorabies virus: A tool for tracing neuronal connections. In: *Protocols for Gene Transfer in Neuroscience. Towards Gene Therapy of Neurological Disorders*, Lowenstein PR, Enquist LW (eds) John Wiley & Sons: Chichester. pp 333–348.
- Enquist LW, Dubin J, Whealy ME, Card JP (1994). Complementation analysis of pseudorabies virus gE and gI mutants in retinal ganglion cell neurotropism. *Journal of Virology* **68**: 5275–5279.
- Gottschall J (1981). The diaphragm of the rat and its innervation. Muscle fiber composition, perikarya and axons of efferent and afferent neurons. *Anatomy and Embryology* **161**: 405–417.
- Grelot L, Milano S, Portillo F, Miller AD (1993). Respiratory interneurons of the lower cervical (C4–C5) cord: membrane potential change during fictive coughing, vomiting, and swallowing in the decerebrate cat. *Pflugers Archives* **425**: 313–320.
- Gustafson DP (1975). Pseudorabies. In: *Diseases of Swine*, Dunne HW, Leman AD (eds) Ames: The Iowa State University Press. pp 391–410.
- Hsu SM, Raine L, Fanger H (1981). The use of avidin-biotin-peroxidase complex (ABC) in immunoperoxidase techniques: a comparison between ABC and unlabeled antibody (PAP) procedures. *Journal of Histochemistry and Cytochemistry* **29**: 577–580.
- Illert M, Lundberg A, Padel Y, Tanaka R (1978). Integration in descending motor pathways controlling the forelimb in the cat. 5. Properties of and monosynaptic excitatory convergence on C3–C4 propriospinal neurones. *Experimental Brain Research* **33**: 101–130.
- Kritas SK, Nauwynck JJ, Pensaert MB (1995). Dissemination of wild-type and gC-, gE- and gI-deleted mutants of Aujeszky's disease virus in the maxillary nerve and trigeminal ganglion of pigs after intranasal inoculation. *Journal of General Virology* **76**: 2063–2066.
- Loewy AD (1995). Pseudorabies virus: A transneuronal tracer for neuronanatomical studies. In: *Viral Vectors*, Kaplitt PG, Loewy AD (eds) Academic Press: San Diego. pp. 349–366.
- McFerran JB, Dow C (1965). The distribution of the virus of Aujeszky's disease (pseudorabies virus) in experimentally infected swine. *American Journal of Veterinary Research* **26**: 631–635.
- McLean IW, Nakane PK (1974). Periodate-lysine-paraformaldehyde fixative. A new fixative for immunoelectron microscopy. *Journal of Histochemistry and Cytochemistry* **22**: 1077–1083.
- Nara PL (1982). Porcine herpesvirus. I. In: *Comparative Pathobiology of Viral Disease*, Olson JR, Krakown S, Blakeslee JJR (eds) CRC Press: Boca Raton. pp 90–113.
- Palisses R, Persegol L, Viala D (1989). Evidence for respiratory interneurons in the C3–C5 cervical spinal cord in the decorticate rabbit. *Experimental Brain Research* **78**: 624–632.
- Rexed B (1954). A cytoarchitectonic atlas of the spinal cord in the cat. *Journal of Comparative Neurology* **100**: 297–380.
- Richmond FJR, Abrams VC (1975). Morphology and distribution of muscle spindles in dorsal muscles of the cat neck. *Journal of Neurophysiology* **38**: 1322–1339.
- Rinaman L, Card JP, Enquist LW (1993). Spatiotemporal responses of astrocytes, ramified microglia, and brain macrophages to central neuronal infection with pseudorabies virus. *Journal of Neuroscience* **13**: 685–702.
- Rose D, Larnicol N, Marlot D, Duron B (1983). Quantitative morphological changes in phrenic and intercostal motor columns and their respective spinal cord segments during postnatal development in the kitten. *Neuroscience Letters*, **40**, 119–125.
- Rotto-Perceley DM, Wheeler JG, Osorio FA, Platt KB, Loewy AD. (1992). Transneuronal labeling of spinal interneurons and sympathetic preganglionic neurons after pseudorabies virus injections in the rat medial gastrocnemius muscle. *Brain Research* **574**, 291–306.
- Sabin AB (1938). Progression of different nasally instilled viruses along different nervous system pathways in the same host. *Proceedings of the Society for Experimental Biology and Medicine* **38**: 270–275.
- Sabo A, Rajcani J, Blaskovic D (1969). Studies on the pathogenesis of Aujeszky's disease. III. The distribution of virulent virus in piglets after intranasal infection. *Acta Virologica*, **13**: 407–414.

- Sternberger LA (1979). *Immunohistochemistry*, 2nd edition, New York: Wiley and Sons.
- Strick PL, Card JP (1992). Transneuronal mapping of neural circuits with alpha herpesviruses. In: *Experimental Neuroanatomy. A Practical Approach* Oxford University Press: Oxford, pp. 81–101.
- Ugolini G (1992). Transneuronal transfer of herpes simplex virus type 1 (HSV 1) from mixed limb nerves to the CNS. I. Sequence of transfer from sensory, motor, and sympathetic nerve fibres to the spinal cord. *Journal of Comparative Neurology* **326**: 527–548.
- Ugolini G (1995). Transneuronal tracing with Alpha-herpesviruses: A review of the methodology. In: *Viral Vectors. Gene Therapy and Neuroscience Applications*, pp. 293–318.
- Willis WD, Coggeshall RE (1991). *Sensory Mechanisms of the Spinal Cord* Plenum Press: New York.
- Watson RE, Wiegand ST, Clough RW, Hoffman GE (1986). Use of cryoprotectant to maintain long-term peptide immunoreactivity and tissue morphology. *Peptides* **7**: 155–159.
- Whealy ME, Card JP, Meade RP, Robbins AK, Enquist LW (1991). Effect of Brefeldin A on alphaherpesvirus membrane protein glycosylation and virus egress. *Journal of Virology* **65**: 1066–1081.
- Whealy ME, Card JP, Robbins AK, Dubin JR, Rziha H-J, Enquist LW (1993). Specific pseudorabies virus infection of the rat visual system requires both gI and gp63 glycoproteins. *Journal of Virology* **67**: 3786–3797.
- Wittmann G, Jakubik J, Ahl R (1980). Multiplication and distribution of Aujeszky's disease (pseudorabies) virus in vaccinated and non-vaccinated pigs after intranasal infection. *Journal of Virology* **66**: 227–240.
- Wittmann G, Rziha HJ (1989). Aujeszky's disease (pseudorabies) in pigs. In: *Herpesvirus Diseases of Cattle, Horses and Pigs*, Wittman G (ed) Kluwer: Boston, pp. 230–325.
- Yates BJ, Jakus J, Miller AD (1993). Vestibular effects on respiratory outflow in the decerebrate cat. *Brain Research* **629**: 209–217.
- Zemanick MC, Strick PL, Dix RD (1991). Direction of transneuronal transport of herpes simplex virus 1 in the primate motor system is strain independent. *PNAS USA* **88**: 8048–8051.